Am J Cancer Res 2024;14(3):979-995
www.ajcr.us /ISSN:2156-6976/ajcr0153927

Original Article

Novel chromium (III)-based compound for inhibition of oxaliplatin-resistant colorectal cancer progression

Ming-Cheng Chen[1,2], Hema Sri Devi[3], Hsueh-Fa Pien[4], Shina Fong-Mei Wen[4], Jenn-Line Sheu[4], Bruce Chi-Kang Tsai[3], Chih-Yang Huang[3,5,6,7,8*], Yu-Jung Lin[3,9*]

[1]Division of Colorectal Surgery, Department of Surgery, Taichung Veterans General Hospital, Taichung, Taiwan; [2]Faculty of Medicine, National Yang Ming Chiao Tung University, Taipei, Taiwan; [3]Cardiovascular and Mitochondrial Related Disease Research Center, Hualien Tzu Chi Hospital, Buddhist Tzu Chi Medical Foundation, Hualien, Taiwan; [4]TOMA Biotechnology Co., Ltd., Taipei, Taiwan; [5]Graduate Institute of Biomedical Sciences, China Medical University, Taichung, Taiwan; [6]Department of Medical Research, China Medical University Hospital, Taichung, Taiwan; [7]Center of General Education, Buddhist Tzu Chi Medical Foundation, Tzu Chi University of Science and Technology, Hualien, Taiwan; [8]Department of Medical Laboratory Science and Biotechnology, Asia University, Taichung, Taiwan; [9]School of Post-Baccalaureate Chinese Medicine, College of Medicine, Tzu Chi University, Hualien, Taiwan. [*]Equal contributors.

Received October 15, 2023; Accepted February 26, 2024; Epub March 15, 2024; Published March 30, 2024

Abstract: Colorectal cancer (CRC) ranks as the third leading cause of cancer-related mortality worldwide. The current standard of care includes systemic chemotherapy with cytotoxic agents, offering palliative relief for severe CRC cases and serving as the primary therapy for metastatic recurrence. However, the development of chemoresistance poses a substantial obstacle in the realm of chemotherapy. This study delved into the potential of a novel chromium (III)-based compound, hexaacetotetraaquadihydroxochromium (III) diiron (III) nitrate, for CRC treatment. The therapeutic promise of this innovative chromium (III)-based compound was explored by utilizing LoVo colon cancer cells and an *in-vivo* mouse model of CRC. Various dosages of the compound were administered to LoVo parental cells and LoVo oxaliplatin-resistant cells. Findings unveiled that a concentration of 2000 μg/mL of the chromium (III) compound significantly inhibited mesenchymal transition and the migratory and invasive properties of LoVo oxaliplatin-resistant cells. This novel chromium (III)-based compound also demonstrated similar efficacy in other different CRC cell lines. The tumor growth was in the *in-vivo* mouse model was reduced by this compound. Moreover, the chromium (III)-based compound induced apoptosis by triggering the endoplasmic reticulum (ER) stress pathway in LoVo oxaliplatin-resistant cells. This study illuminates the capacity of the novel chromium (III)-based compound to impede the progression and growth of chemotherapy-resistant CRC. This discovery instills confidence in the potential of this compound as a therapeutic agent for CRC, even in the face of drug resistance. It holds the promise of serving as a valuable asset in the future treatment of chemotherapy-resistant CRC.

Keywords: Hexaacetotetraaquadihydroxochromium (III) diiron (III) nitrate, chromium (III)-based compound, oxaliplatin-drug resistant, apoptosis, colorectal cancer

Introduction

Colorectal cancer (CRC) remains a formidable global health challenge, contributing substantially to mortality rates worldwide. While advancements in cancer interventions have led to a decline in CRC incidence and mortality, the emergence of drug resistance poses an obstacle. Furthermore, the number of younger individuals being diagnosed with colon cancer is concerningly increasing. The intricate interplay of environmental and genetic factors continues to play a pivotal role in the initiation and progression of colon cancer. Efforts to address these challenges and enhance therapeutic strategies are crucial for further progress in managing this complex malignancy [1]. Platinum-based cancer chemotherapy, particularly the use of oxaliplatin, stands as a primary treatment for CRC [2].

Oxaliplatin, which is a third generation of platinum-based derivative, functions as an alkylating agent [3]. The platinum complex within oxali-

https://doi.org/10.62347/XTRT2780

platin covalently attaches to DNA, generating platinum-DNA adducts that hinder DNA replication and transcription, leading to cell cycle arrest and cell death [4, 5]. Oxaliplatin is widely utilized in the first-line chemotherapy of CRC and has proven effective in treating stages III and IV CRC [6]. Several studies have substantiated its considerable therapeutic efficacy, underscoring its role in managing CRC [7]. However, resistance to oxaliplatin commonly develops in CRC cells due to prolonged usage, and it becomes a challenging issue [8]. The mechanisms of oxaliplatin resistance in CRC cells are complex. Previous studies have shown the involvement of certain mechanisms in CRC cells resistant to oxaliplatin. For example, the circular RNA circHIPK3 exhibits increased expression in patients with chemotherapy-resistant CRC and contributes to oxaliplatin resistance by serving as a miR-637 sponge. This action suppresses autophagy-related cell death through the modulation of the STAT3/Bcl-2/beclin1 axis [9]. Similarly, the upregulation of the transcription factor FOXC1 leads to its binding to the miR-31 promoter, subsequently enhancing the expression of miR31-5p. This modulation, in turn, influences the expression of LATS2, contributing to the resistance of CRC cells to oxaliplatin [6]. The transcription factor NF-κB boosts the expression of ABCG2, diminishing the effectiveness of oxaliplatin in CRC cells. This phenomenon occurs through the attenuation of endoplasmic reticulum (ER) stress-induced apoptosis [10]. Aurora-A, with functions as an oncogene, exhibits increased expression in CRC cells resistant to oxaliplatin. It contributes to oxaliplatin resistance by suppressing p53 signaling in CRC cells [11]. Despite not fully understanding the mechanisms underlying oxaliplatin resistance in CRC cells, the quest for safe and effective novel drugs with lower toxicity and fewer side effects is vital to assist patients dealing with drug-resistant colon cancer.

Chromium is a micronutrient existing in the environment, with its primary oxidation states being trivalent and hexavalent. Trivalent chromium is generally considered non-toxic, but hexavalent chromium poses a toxic and is classified as a carcinogen for the human body [12]. Exposure to hexavalent chromium significantly increases the risk of various cancers in the mouth, pharynx, respiratory system, stomach, and prostate in the human body [13]. Meanwhile, trivalent chromium, exemplified by chromium picolinate, can be applied as a micronutrient and a nutritional supplement. It offers various health benefits to animals and humans, and it is considered a pharmacologically active element in appropriate doses [12]. Supplementing with chromium (III)-based compounds could alleviate insulin resistance and contribute to lowering the risk of various types of diabetes [14]. Numerous innovative compounds based on chromium (III) have been synthesized to address various diseases. For instance, a compound combining genistein and chromium (III) demonstrated effective hypoglycemic activity in db/db diabetic mice, without exhibiting potential toxicity in normal mice [15]. A polysaccharide-linked chromium (III)-based compound was employed safely to diminish hyperlipidemia production and alleviate inflammatory infiltration induced by hyperlipidemia [16]. In cancer research, the in-situ transition system from chromium (V) to chromium (III) enhanced oxidative stress generation, resulting in efficient cancer therapy in *in-vivo* and *in-vitro* settings [17]. A synthesized chromium (III)-containing compound showed potential to decrease the occurrence of colorectal tumors induced by 1,2-dimethylhydrazine in male Sprague-Dawley rats [18]. Due to their potential medical value, the development of novel chromium (III)-based compounds has potential to serve as a therapy for diminishing drug-resistant colon cancer.

As mentioned before, drug resistance is a critical hurdle in the therapeutic approach to CRC. Hence, the imperative lies in the development of novel drugs and strategic interventions to effectively combat resistance in treating CRC. Hexaacetotetraaquadihydroxochromium (III) diiron (III) nitrate (**Figure 1**), which is a novel chromium (III)-based compound that has potential to prevent and treat SARS-CoV-2 virus [19], was investigated in the present study for its effectiveness in treating CRC. This study aimed to elucidate the mechanism by which this compound inhibits CRC development. The results revealed that the compound primarily induces apoptosis in oxaliplatin-resistant CRC tumors through the ER-stress pathway.

Material and method

Chemicals, reagents, drugs, and antibodies

All chemicals and reagents utilized in the study were of research-grade quality and were pro-

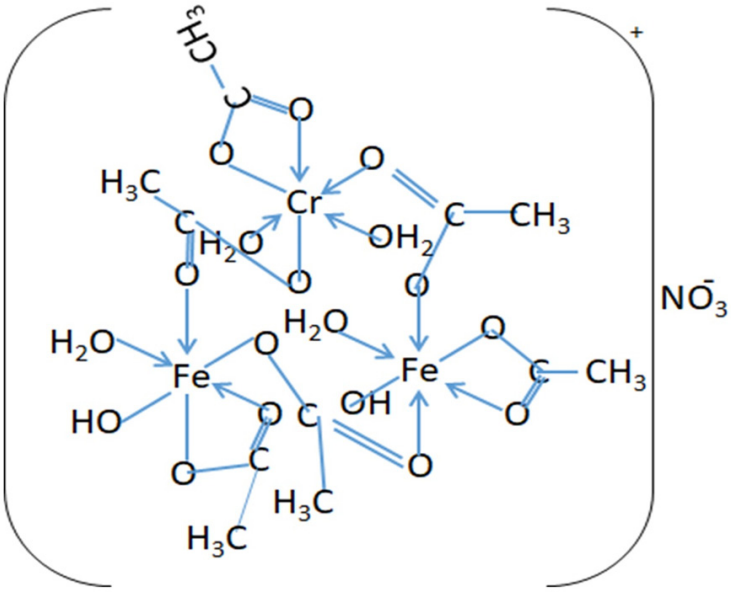

Figure 1. Chemical structure of the novel chromium (III)-based compound [hexaacetotetraaquadihydroxochromium (III) diiron (III) nitrate].

cured from Merck (Darmstadt, Germany) and Sigma-Aldrich (St. Louis, MO, USA). The innovative chromium (III)-based compound, provided by TOMA BIO. Co., Ltd. (Taipei, Taiwan), is a chromium (III) derivative. This compound is identified as hexaacetotetraaquadihydroxochromium (III) diiron (III) nitrate, featuring the chemical formula $[CrFe_2(CH_3CO_2)_6(H_2O)_4(OH)_2]^+ NO_3^-$, a molecular formula of $CrFe_2C_{12}H_{28}NO_{21}$, and a molecular weight of 686.11 g/mol. Oxaliplatin (O9512), 5-FU (F6627), and irinotecan hydrochloride (I1406) were procured from Sigma-Aldrich. The primary antibodies GAPDH (sc-32233), PERK (sc-377400), and vimentin (sc-32322) were sourced from Santa Cruz Biotechnology Inc. (Santa Cruz, CA, USA). The primary antibodies ATF4 (#11815), CHOP (#2895), cleavage caspase-3 (#9664), E-cadherin (#3195), eIF2-α (#9722), phospho-eIF2α (Ser51, #9721), and PARP (#9542) were purchased from Cell Signaling Technology (Danvers, MA, USA).

Cell culture

LoVo (60148, $LoVo^{Parental}$ cell line), SW620 (60343), HCT-116 (60349), and H9c2(2-1) cell lines (60096) were obtained from Bioresource Collection and Research Center in Hsinchu, Taiwan. The culture medium of LoVo cell line was low-glucose Dulbecco's Modified Eagle's Medium (DMEM, D55-23, Sigma-Aldrich, Saint Louis, MO, USA). The culture medium of SW620 cell line was Leibovitz's L-15 medium (L4386, Sigma-Aldrich). The culture medium of HCT-116 cell line was McCoy's 5A medium with 1.5 mM L-glutamine (CM1043, ACE Biolabs, Taoyuan, Taiwan). The culture medium of H9c2(2-1) cell line was high-glucose DMEM (D7777, Sigma-Aldrich). These media were supplemented with 10% HyClone-characterized fetal bovine serum (SH30071.03, Cytiva, Marlborough, MA, USA) and 100 U/mL penicillin-streptomycin (15140122, Thermo Fisher Scientific, Waltham, MA, USA) for cell culture. Beas-2B cell line (CRL-3588) was purchased from American Type Culture Collection (Manassas, VA, USA) and plated in LHC-9 serum-free medium (1268-0013, Thermo Fisher Scientific) with 100 U/mL penicillin-streptomycin (Thermo Fisher Scientific). All cell cultures were maintained in a humidified atmosphere with 5% CO_2 at 37°C.

Establishment of oxaliplatin-resistant LoVo ($LoVo^{OXAR}$) CRC cells

To generate stable oxaliplatin-resistant CRC cells ($LoVo^{OXAR}$), LoVo cells (1×10^6) were seeded in 10 cm plates with oxaliplatin dose-dependent exposure ranging from 0 μg/mL to 25 μg/mL for 24 h of incubation to generate stable $LoVo^{OXAR}$ CRC cells. The exposure resulted in 50% cell death with oxaliplatin IC_{50} at 15 μg/mL in $LoVo^{Parental}$ CRC cells. Subsequently, the surviving cells were allowed to reach 80% confluence, followed by two successive passages at the same concentration with continued oxaliplatin treatment. The same procedure was repeated with increasing oxaliplatin doses (15-60 μg/mL). Following these treatments, the $LoVo^{OXAR}$ cell population with a fourfold higher

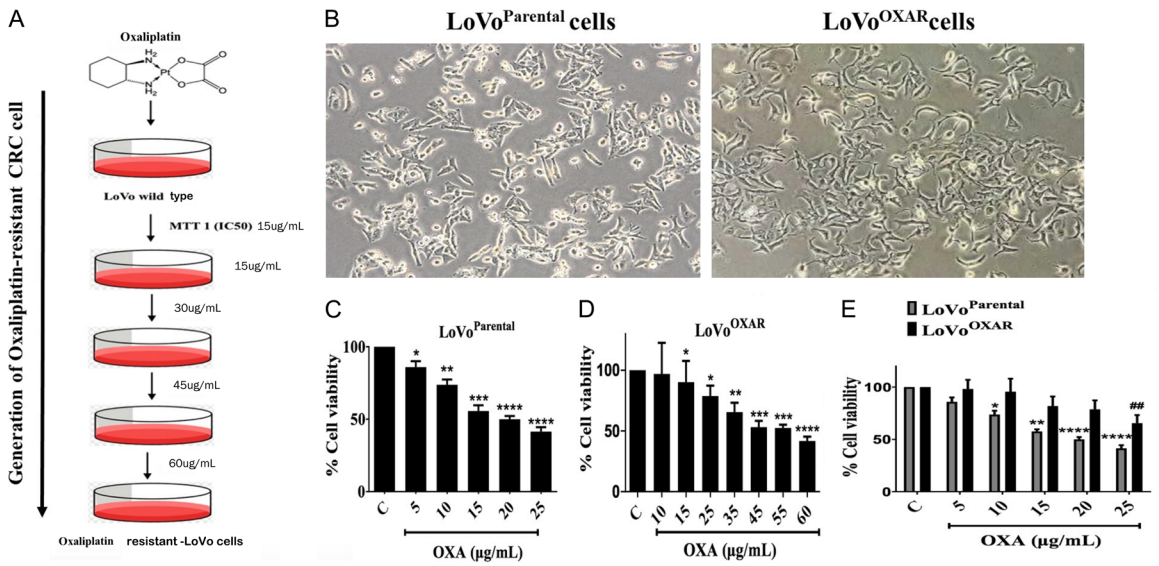

Figure 2. Establishment and characterization of oxaliplatin-resistant LoVo colorectal cancer cell line. A. Stable oxaliplatin resistance was maintained by exposing colorectal cancer cell lines to oxaliplatin (0-25 μg/mL) for 24 h, which resulted in 50% cell death at 15 μg/mL in colorectal cancer cell lines. The procedure was repeated until a fourfold greater IC_{50} (60 μg/mL) oxaliplatin resistance was established. B. Distinct morphological characteristics between the $LoVo^{parental}$ and $LoVo^{OXAR}$ cell lines were observed under 20 × magnification. C and D. MTT assay was used to determine the IC_{50} values of the oxaliplatin-treated $LoVo^{parental}$ and $LoVo^{OXAR}$ colorectal cancer cell lines. The IC_{50} values of $LoVo^{parental}$ and $LoVo^{OXAR}$ cells were 15 and 60 μg/mL, respectively. The data were expressed mean ± standard deviation (SD, n = 3). *P < 0.05, **P < 0.01, ***P < 0.001 versus ****P < 0.0001 versus control. E. The resistance of the two cell lines to oxaliplatin was compared. *P < 0.05 versus $LoVo^{parental}$ cells and ##P < 0.01 $LoVo^{parental}$ versus oxaliplatin-resistant LoVo cells.

IC_{50} (60 μg/mL) to oxaliplatin than the parental cell lines was selected (**Figure 2A**). The $LoVo^{OXAR}$ cell line was cultured in low-glucose DMEM (D5523, Sigma-Aldrich) with 10% HyClone-characterized FBS (SH30071.03, Cytiva) and 100 U/mL penicillin-streptomycin (15140122, Thermo Fisher Scientific) in a humidified atmosphere with 5% CO_2 at 37°C.

3-(4, 5-Dimethylthiazol-2-yl)-2, 5-diphenyltetrazolium-bromide (MTT) assay

MTT assay was employed to assess cell viability. MTT (475989) dissolved in water was obtained from Sigma-Aldrich. Cells were initially plated in 96-well plates at a density of 1 × 10^4 cells per well and cultured in triplicate in suggested culture media for 24 h in 24-well plates. Subsequently, they were exposed to the respective drugs under experimental conditions. After 24 h of treatment, the medium was aspirated, and 100 μL of MTT solution (5.0 mg/mL) was added to each well, followed by an incubation period of 4 h at 37°C until a purple precipitate developed. Post-incubation, the supernatant was removed, and 150 μL of DMSO was added to dissolve the blue MTT formazan crystals. Absorbance at 570 nm was measured using a multi-well ELISA plate reader (Molecular Devices, Palo Alto, CA, USA). The IC_{50} value, which represents the concentration causing 50% cell death, was determined. Cell survival percentage was calculated using the following formula: Cell survival (%) = ($OD_{experimental\ sample}$ - blank/$OD_{control\ sample}$ - blank) × 100% (n = 3) [20].

Immunofluorescence staining

$LoVo^{Parental}$ cells or $LoVo^{OXAR}$ cells were initially seeded in an eight-well Nunc Lab-Tek Chamber Slide (177402, Thermo Fisher Scientific) at a density of 1 × 10^4 cells per well and cultured in low-glucose DMEM supplemented with 10% FBS. Following incubation, the cells were fixed with 4% paraformaldehyde in 1 × PBS for 1 h at 25°C. Subsequently, each well received 0.5 mL of permeabilization solution (0.1% Triton X-100 in 0.1% sodium citrate), and the plates were placed on ice for 2 min without agitation. Then, 1 mL of 2% BSA blocking buffer was introduced to each well to minimize nonspecific binding. For immunostaining, a diluted primary antibody

solution (1:100, 500 μL) was added to each well and incubated for 12 h at 4°C. Afterwards, the primary antibody was removed and washed twice with 1 × PBS. Subsequently, suitably diluted Invitrogen fluorescent secondary antibody (1:100, 500 μL, Thermo Fisher Scientific) was added into each well and incubated in the dark for 1 h at 25°C. Then, all wells were washed twice with 1 × PBS. 4',6-Diamidino-2-phenylindole (DAPI, 500 μL, diluted 10,000 ×, 62248, Thermo Fisher Scientific) was added to each well, and the plates were incubated for 30 min at 25°C in the dark to stain cell nuclei. Then, they were washed thrice with 1 × PBS. The fluorescent intensity of the cells was examined using an Olympus CKX53 microscope (Olympus Corporation, Shinjuku-ku, Tokyo, Japan).

Transwell migration and invasion assay

A total of 5 × 10^4 cells were suspended in 200 μL serum-free culture medium and placed into the upper compartment of a Corning Transwell chamber (3422, Corning, NY, USA; 24-well insert, pore size: 8 μm). The lower chamber was filled with culture medium containing 10% FBS, serving as an attractant. Subsequently, the cells were incubated at 48 h for migration and invasion assays. In the case of invasion assay, the inserts were pre-coated with Corning® matrigel basement membrane matrix (CLS-354234, Sigma-Aldrich). At the end of each experiment, the cells on the upper surface of the membrane were eliminated, and the lower surface was fixed and stained with 0.5% crystal violet (ab143095, abcam, UK). The cells in five randomly selected areas were counted using a microscope (× 200). The invasion and migration rates were determined using the following formula: Invasion or migration rate (%) = (average number of transmembrane cells in the treatment group/average number of transmembrane cells in the control group [no treatment]) × 100% [21].

Real-time PCR (RT-PCR) assay

Total RNA was isolated from cells by using a GeneJET RNA purification kit (K0732, Thermo Fisher Scientific). Subsequently, reverse transcription to cDNA was carried out using a GScript First-Strand Synthesis Kit (MB305-0050, GeneDireX, Taoyuan, Taiwan) following the manufacturer's protocol. RT-PCR was conducted using ORA SEE qPCR Green ROX L Mix (QPD0501, highQu GmbH, Kraichtal, Germany), and melting curve analysis was conducted in accordance with the instructions from the instrument kit. Primers targeting epithelial-mesenchymal transition (EMT) markers (TJP1, FN1, E-cadherin, and vimentin) were synthesized by Protech Technology Enterprise Co., Ltd. (Taipei, Taiwan), with the following sequences: E-cadherin, forward: 5'-CCC GGG ACA ACG TTT ATT AC-3', reverse: 5'-GCT GGC TCA AGT CAA AGT CC-3'; vimentin, forward: 5'-TCC AGC AGC TTC CTG TAG GT-3', reverse: 5'-GAG AAC TTT GCC GTT GAA GC-3'; fibronectin 1 (FN1), forward: 5'-GAC GCA TCA CTT GCA CTT CT-3', reverse: 5'-GCA GGT TTC CTC GAT TAT CCT-3'; TJP1, forward: 5'-CCA GCT GGT ATG GGT TTC C-3', reverse: 5'-TCT ACT GTC CGT GCT ATA CAT TGA GT-3'; and GAPDH, forward: 5'-GCA CCG TCA AGG CTG AGA AC-3', reverse: 5'-ATG GTG GTG AAG ACG CCA GT-3', used as an endogenous control. The $2^{-\Delta\Delta Ct}$ method was employed for the determination of the relative levels of gene transcripts, which were subsequently normalized to GAPDH [22, 23]. The experimental results were examined using the QuantStudio 5 Real-Time PCR system (Thermo Fisher Scientific).

Western blot analysis

Cell samples were treated with RIPA buffer for 30 min on ice and centrifuged at 13,000 rpm for 60 min at 4°C to collect the supernatants. The protein concentration in each sample was measured using a Bio-Rad protein assay kit (5000006, Bio-Rad Laboratories, Hercules, CA, USA). The aliquots of protein from each tissue sample were combined with suitable quantities of 5 × loading dye, followed by 5 min incubation at 95°C. The same amount of whole-cell lysate (30 μg) from each sample was separated by 10%-12% sodium dodecyl sulfate-polyacrylamide gels at 80-100 V for a specific duration. Following electrophoresis, proteins were transferred onto a polyvinylidene difluoride membrane (IPVH85R, Merck Millipore, Bedford, MA, USA) by using a Bio-Rad transfer system (Bio-Rad Laboratories). The membranes were then incubated with primary antibodies (1:1000 dilution) at 4°C overnight, followed by 1 h incubation with appropriate horseradish peroxidase-labeled secondary antibodies (1:10000 dilution, Santa Cruz Biotechnology) at 25°C. Protein signals were visualized using Immobilon

Western HRP substrates (WBKLS0500, Merck Millipore) on an Image Bright i500 imaging system (Invitrogen iBright Imaging System, Thermo Fisher Scientific). Densitometry analysis was carried out using ImageJ software (version 1.50, National Institutes of Health, Bethesda, MD, USA) [24, 25]. GAPDH was served as the endogenous control for the normalization of protein amounts.

Terminal deoxynucleotidyl transferase dUTP nick-end labeling (TUNEL) assay

Cell apoptosis was assessed using an in-situ cell death detection kit (11684795910, Roche Applied Science, Penzberg, Upper Bavaria, Germany). Nuclei were counterstained with DAPI (Thermo Fisher Scientific). TUNEL-positive cells were visualized using an Olympus CKX53 microscope (Olympus Corporation) [26].

Nude mouse cancer tumor model

All experiments were conducted in compliance with the guidelines and approval from the Institutional Animal Care and Ethics Committee of Hualien Tzu Chi Hospital (Hualien, Taiwan) with consent approval number 110-41, adhering to the Guide for the Care and Use of Laboratory Animals by NIH. Male NU/NU mice, approximately 12 in number and weighing 20-22 g at 6 weeks of age, were procured from Bio LASCO Taiwan Co., Ltd. (Taipei, Taiwan). The NU/NU nude mice were housed in a controlled environment with a temperature of 25°C ± 1°C and a relative humidity of 55% at Tzu-Chi University Animal Center. They were divided into four groups, each comprising five mice. CRC cells (1×10^6) in 100 µL Corning Matrigel Matrix (CLS354234, Sigma, Corning, NY, USA) were subcutaneously injected into the legs of NU/NU mice. The experimental design included four groups. Groups 1 and 2 received injections of $LoVo^{parental}$ cells. Group 1 served as a control with no treatment (LoVo CRC tumor), whereas group 2 was orally treated with the chromium (III)-based compound in PBS (100 mg/kg/day, 5 days/week for 3 weeks). Group 3 received injections of $LoVo^{OXAR}$ cells without any treatment. Group 4 was injected with LoVo-OXAR cells and orally treated with the chromium (III)-based compound in PBS (100 mg/kg/day, 5 days/week for 3 weeks). Seven days after tumor inoculation (when the tumor volume reached a size range of 50-100 mm^3), the mice were orally administered with the chromium (III)-based compound daily for 3 weeks. The tumor volume was measured every 3 days by using a caliper and calculated using the formula [(L × W × W)/2], where L and W are the length and width, respectively. All mice were euthanized after treatment, and the tumors were excised and weighed.

MTS assay

In the presence of phenazine methosulfate, MTS is bio-reduced by viable cells into a formazan product that is soluble in culture media. A total of 6×10^3 cells/well were seeded in a 96-well µL plate, with a final volume of 200 µL/well. Subsequently, the cells were exposed to the respective drugs on the basis of the experimental conditions. After 24 h of treatment, 20 µL/well of MTS reagent (G3581, Promega, Madison, WI, USA) was added into each well. Then, the plate was incubated for 4 h at 37°C in standard culture conditions. The plate was shaken briefly on a shaker, and the absorbance of the treated and untreated cells was measured at 490 nm by using a multi-well ELISA plate reader (Molecular Devices, Palo Alto, CA, USA). The IC_{50} value, representing the concentration causing 50% cell death, was determined. The cytotoxic effect (V_R) was calculated using the following equation: $V_R = A/A_0 \times 100\%$ (n = 3), where A and A_0 are the absorbance of the experimental and control groups, respectively.

Statistical analysis

Each sample was analyzed on the basis of experiments that were repeated at least three times. Statistical significance was evaluated using SigmaPlot (version 10.0, Systat Software Inc., San Jose, CA, USA). Student's *t*-test was utilized to assess the significance between two groups, and one-way ANOVA was employed for statistical analyses involving multiple groups. Statistical significance was defined as differences with $P < 0.05$.

Results

Establishment of oxaliplatin resistance in CRC cells

Oxaliplatin is a widely recognized chemotherapeutic agent that hinders the proliferation of tumor cells through the formation of DNA-platinum adducts, ultimately resulting in the death of cancer cells [4, 5]. However, drug

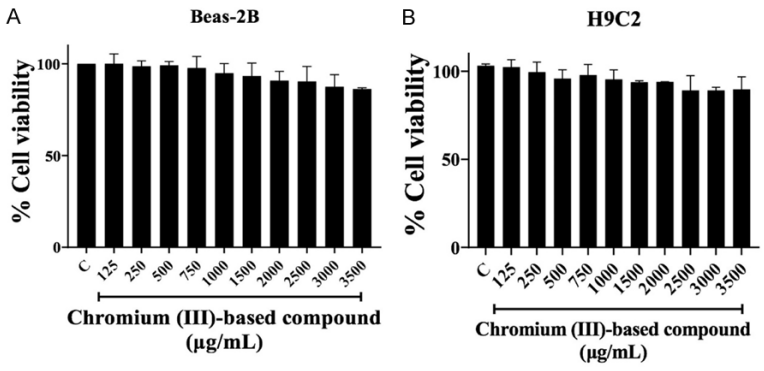

Figure 3. Toxicity of chromium (III)-based compound in normal cells. The toxicity of the chromium (III)-based compound was evaluated by MTS assay using Beas-2B (human lung epithelial cells) and H9c2 (rat myoblast). The results revealed that concentrations above 2500 μg/mL displayed minimal toxicity in both cell lines, whereas no notable cytotoxic effects were observed at lower doses. The data were expressed as mean ± standard deviation (SD, n = 3). *P < 0.05 versus control.

resistance remains a major issue for the efficacy and tolerability of this therapeutic strategy [8]. Thus, a CRC cell line resistant to oxaliplatin was established to address the issue.

Oxaliplatin-resistant CRC cells (LoVo^{OXAR} cells) were established for further study by incubating LoVo cells (1 × 10^6/well) at 24 h treatment in an oxaliplatin dose-dependent manner (0, 5, 10, 15, 20, and 25 μg/mL). The IC_{50} was determined to be 15 μg/mL. The surviving cells were continually maintained with oxaliplatin and allowed to grow to 80% confluence before passage. The procedure was repeated by increasing the oxaliplatin concentrations by at least fourfold greater IC_{50} (60 μg/mL) to oxaliplatin resistance than the LoVo^{parental} cells (**Figure 2A**). The morphology of LoVo^{parental} and LoVo^{OXAR} cells under 20 × magnification displayed distinct characteristics. The LoVo^{parental} cells exhibited a tubular shape with evident cell-cell contact, whereas the LoVo^{OXAR} cells had a more mesenchymal shape, with a flattened cobblestone long-shaped appearance and showed grouped cells without tight cell-cell contacts (**Figure 2B**). Subsequently, the increased resistance of LoVo^{OXAR} cells to oxaliplatin compared with that of LoVo^{parental} cells was confirmed. By using the MTT method, the IC_{50} values of oxaliplatin on the LoVo^{parental} and LoVo^{OXAR} cells were determined to be 15 and 65 μg/mL, respectively (**Figure 2C-E**). These findings showed that the established oxaliplatin-resistant LoVo CRC cells can be classified as drug-resistant cells.

Enhancement of chemotherapeutic efficacy and inhibition of metastasis in parental and oxaliplatin-resistant CRC cells by chromium (III)-based compound

The newly developed compound, hexaacetotetraaquadihydroxochromium (III) diiron (III) nitrate, is identified as a derivative of chromium (III), as shown in **Figure 1**. This study mainly aimed to examine the influence of the new chromium (III)-based compound on drug resistance in CRC cells. Initially, the safety profile of the chromium (III)-based compound was examined. The toxicity of the compound was assessed using Beas-2B (human lung epithelial cells) and H9c2 (rat myoblast) through MTS assay. The findings indicated that concentrations exceeding 2500 μg/mL exhibited minimal toxicity in both cell lines, with no significant cytotoxic effects observed at lower doses (**Figure 3A** and **3B**). Afterwards, the effect of the chromium (III)-based compound on CRC cells was examined.

A dose-dependent inhibition of viability was observed in LoVo^{parental} and LoVo^{OXAR} CRC cells upon treatment with the chromium (III)-based compound. The cell viability significantly decreased, causing 50% cell death at concentrations of 500 and 2000 μg/mL for LoVo^{parental} and LoVo^{OXAR} cells, respectively (**Figure 4A-C**). The combined effect of the chromium (III)-based compound with oxaliplatin and other chemotherapeutic drugs (5-FU and irinotecan) on LoVo^{parental} and LoVo^{OXAR} cells was evaluated to explore potential synergies. The chromium (III)-based compound significantly enhanced the efficacy of these chemotherapeutic drugs (**Figure 4D**). In addition, the chromium (III)-based compound inhibited the metastasis of CRC cell lines in a dose-dependent manner. Vimentin and E-cadherin are molecular markers linked to tumor progression through their roles in EMT, which is a pathological process that contributes to cancer progression, particularly invasion and migration [27-29]. Vimentin is a key component of the intermediate filament that helps maintain cellular integrity and resis-

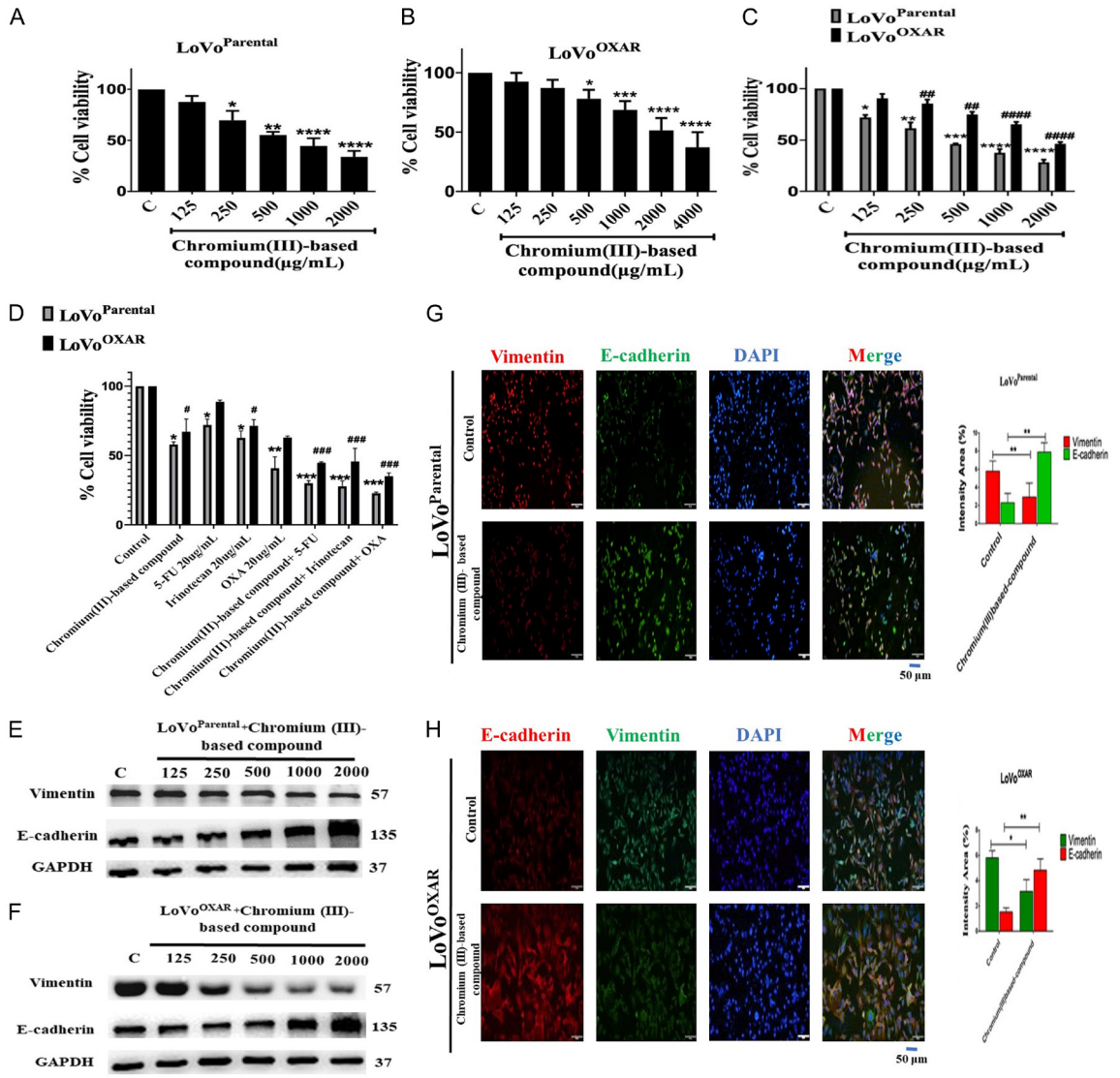

Figure 4. Ability of chromium (III)-based compound to suppress colorectal cancer cells. A and B. MTT assay was used to determine the IC_{50} values of LoVo^{parental} and LoVo^{OXAR} colorectal cancer cell lines treated with the chromium (III)-based compound for 24 h. The IC_{50} values of LoVo^{parental} and LoVo^{OXAR} colorectal cancer cell lines were 500 and 2000 μg/mL, respectively. C. The two cell lines were compared. *P < 0.05, **P < 0.01, ***P < 0.001, and ****P < 0.0001 versus the control group of LoVo^{parental}, and ##P < 0.01, and ####P < 0.0001 LoVo^{parental} versus LoVo^{OXAR} colorectal cancer cells. D. Clinical drugs were used as follows: oxaliplatin; 20 μg/mL, 5-FU; 20 μg/mL, and irinotecan; 20 μg/mL. The synergetic effect of the chromium (III)-based compound when combined with clinical drugs significantly inhibited the viability of LoVo^{parental} [200 μg/mL chromium (III)-based compound with 5 μg/mL oxaliplatin] and LoVo^{OXAR} [500 μg/mL chromium (III)-based compound with 20 μg/mL oxaliplatin] colorectal cancer cell lines. The clinical drugs that inhibited the development of colorectal cancer cell lines were made more effective by the chromium (III)-based compound. Significance is denoted as *P < 0.05 and ***P < 0.001 versus the control group of LoVo^{parental} cells, and #P < 0.05 and ###P < 0.001 versus the control group of LoVo^{OXAR} cells. E-H. Epithelial-mesenchymal transition markers (E-cadherin and vimentin) were determined using immunofluorescence staining and western blot. GAPDH was used as an internal control. The scale bar was 50 μm. The data were expressed as mean ± standard deviation (SD, n = 3). *P < 0.05, **P < 0.01 versus control group.

tance to stress [28]. E-cadherin maintains epithelial phenotypes by mediating the contact inhibition of proliferation when cells reach confluence, and it is known as a tumor suppressor [29, 30]. Western blot and immunofluorescence staining were performed to determine the EMT markers in the LoVo^{parental} and LoVo^{OXAR} CRC cell lines. The results of Western blot

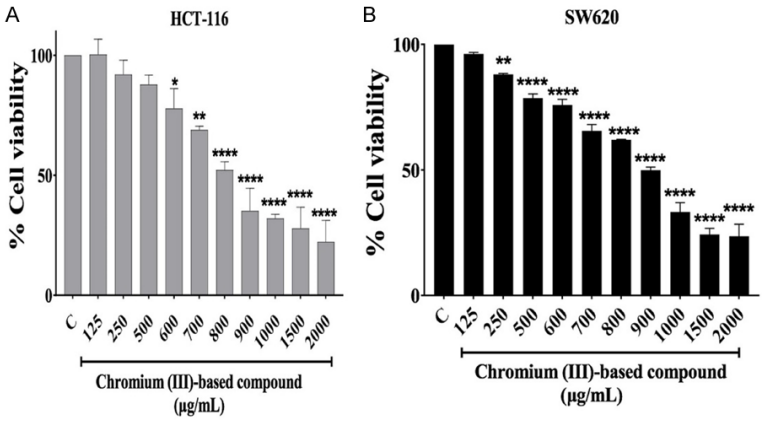

Figure 5. Efficacy of chromium (III)-based compound to limit the viability of SW620 and HCT-116 colorectal cancer cell lines. A and B. SW620 and HCT-116 colorectal cancer cell lines were incubated with the chromium (III)-based compound for 24 h, and the inhibitory rates were measured by MTT assay. The SW620 and HCT-116 colorectal cancer cells reached the IC_{50} values of cell viability at 900 and 800 μg/mL, respectively. The data were expressed as mean ± standard deviation (SD, n = 3). *P < 0.05, **P < 0.01, ***P < 0.001, and ****P < 0.0001 versus control.

revealed a significant reduction in the vimentin protein levels and an increase in the E-cadherin protein levels upon treatment with the chromium (III)-based compound (**Figure 4E** and **4F**). The intensity area demonstrated that the compound reduced tumor metastasis by suppressing the vimentin protein marker (**Figure 4G**), whereas the E-cadherin expression increased (**Figure 4H**). Moreover, two additional CRC cell lines, namely, SW620 and HCT-116, were employed to validate the anti-CRC efficacy of the chromium (III)-based compound and enhance the reliability of the experiment. The results demonstrated that the chromium (III)-based compound suppressed the viability of both CRC cell lines (**Figure 5A** and **5B**). The SW620 and HCT-116 CRC cells exhibited IC_{50} values for cell viability at 900 and 800 μg/mL, respectively. The results indicated that the chromium (III)-based compound has potential as a therapy by augmenting the effectiveness of chemotherapy in suppressing CRC growth and the ability of metastasis in CRC.

Inhibition of migration and invasion in parental and oxaliplatin-resistant CRC cells by chromium (III)-based compound

A comprehensive approach involving RT-PCR and Transwell migration and invasion assays was employed to further elucidate the effect of the chromium (III)-based compound on the metastatic ability of CRC cells. The RT-PCR results revealed a notable increase in the E-cadherin and TJPI mRNA expression levels and a decrease in the vimentin and FN1 expression levels in $LoVo^{parental}$ and $LoVo^{OXAR}$ cells following treatment with the chromium (III)-based compound (**Figure 6A** and **6B**). TJP1, identified as a scaffold tight junction protein 1, is indicative of an epithelial cell characteristic that diminishes during EMT and cancer development [31, 32]. However, in some cases, altered expression or function of tight junction proteins has been implicated in various cancers. Changes in cell adhesion and junctional complexes can contribute to tumor progression and invasion [33, 34]. On the contrary, FN1 plays a key role in the occurrence and development of various tumors and acts as a key gene in gastric cancer [35-37]. Additional research was conducted to further delve into the role of the chromium (III)-based compound in metastasis, particularly its potential to inhibit cancer cell migration and invasion. Transwell assay, which is widely employed for testing tumor progression, migration, and invasiveness, was utilized. The $LoVo^{parental}$ and $LoVo^{OXAR}$ cells were treated with the chromium (III)-based compound for migration (48 h) and invasion (72 h). The results demonstrated a significant inhibition of migration and invasion in both cell lines compared with oxaliplatin treatment alone (**Figure 6C** and **6D**). Remarkably, the combination of the chromium (III)-based compound with oxaliplatin exhibited complete elimination of tumor progression during the migration and invasion phases. Moreover, the compound decreased the migratory capabilities of SW620 and HCT-116 CRC cell lines, and its synergistic combination with oxaliplatin strengthened the efficacy (**Figure 7**). The findings suggested that the chromium (III)-based compound not only effectively inhibits the viability of CRC cells but also hinders their ability to migrate and invade in parental and oxaliplatin-resistant CRC cells.

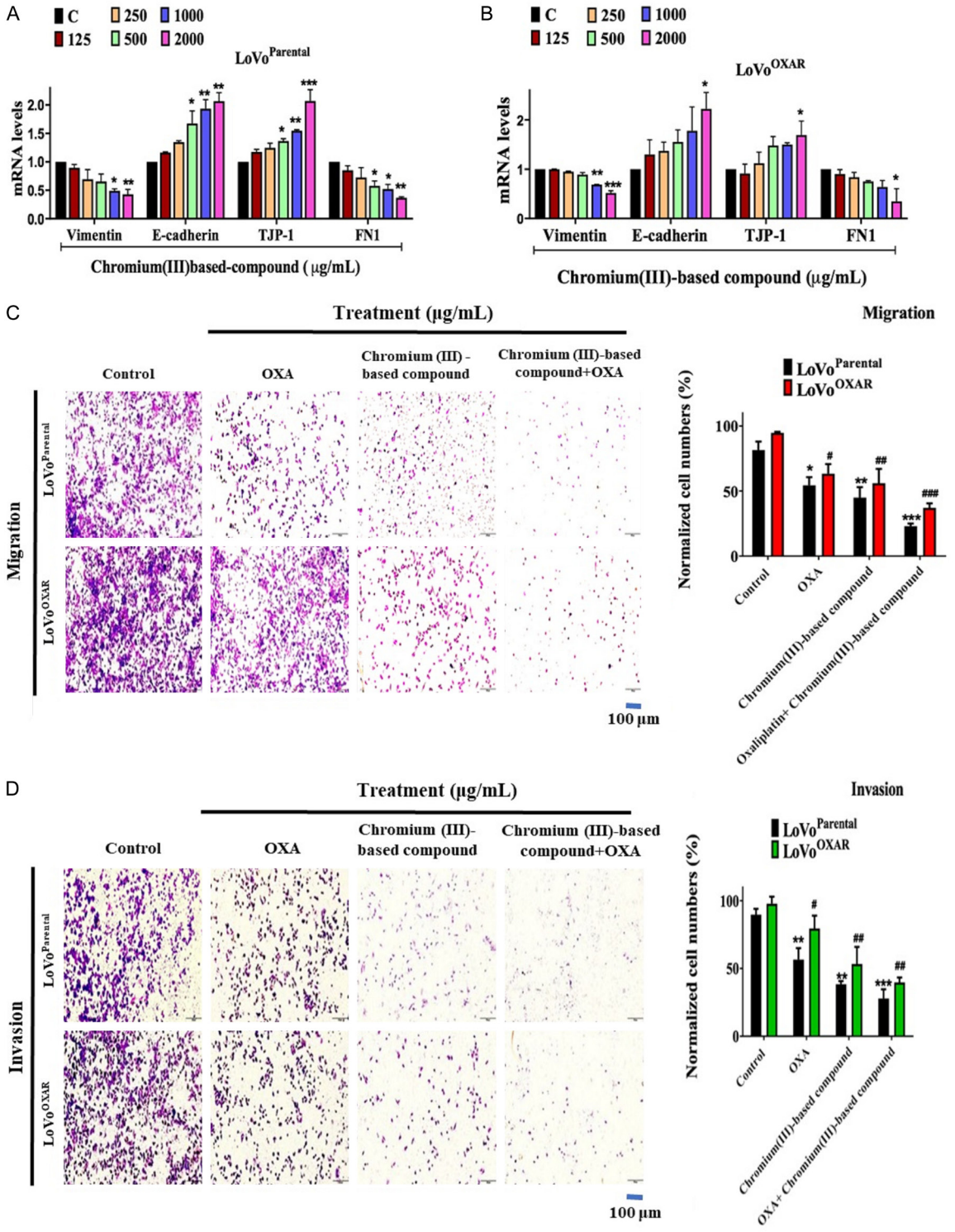

Figure 6. Inhibition of migration and invasion of LoVo^{parental} and LoVo^{OXAR} colorectal cancer cell lines by chromium (III)-based compound. A and B. Epithelial-mesenchymal transition markers (TJP1, FN1, E-cadherin, and vimentin) were determined using RT-PCR. C. Cell migration was detected in LoVo^{parental} and LoVo^{OXAR} colorectal cancer cell lines by using transwell assay. D. Cell invasion was detected in LoVo^{parental} and LoVo^{OXAR} colorectal cancer cell lines using invasion assay. The data are shown as the mean ± standard deviation (SD) of three replicates. *P < 0.05, **P < 0.01, and ***P < 0.001 compared with the control group of LoVo^{parental} cells. #P < 0.05, ##P < 0.01, and ###P < 0.001 compared with the control group of LoVo^{OXAR} cells. The scale bar was 100 μm.

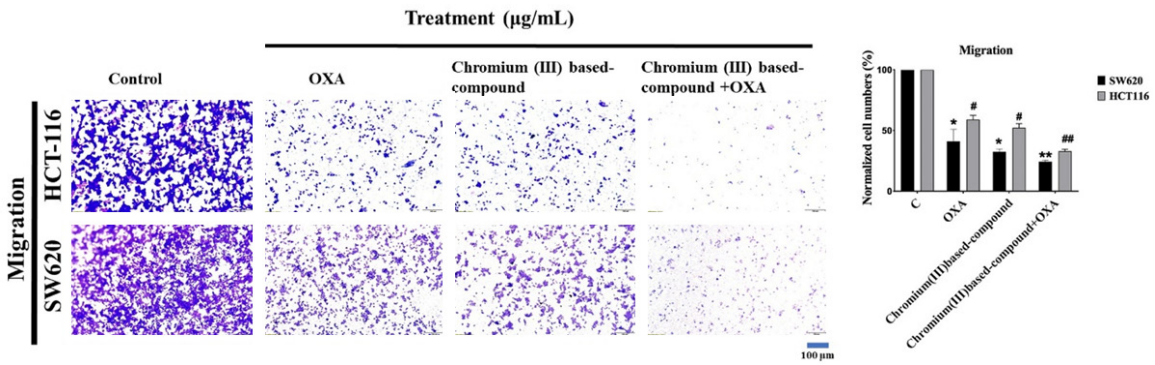

Figure 7. Inhibition of HCT-116 and SW620 colorectal cancer cell migration by the chromium (III)-based compound. The chromium (III)-based compound inhibited the migration ability of colorectal cancer cells. HCT-116 and SW620 colorectal cancer cells were incubated with the chromium (III)-based compound in a dose-dependent manner for 48 h, and the migration rates were measured by transwell assay. The HCT-116 cells were incubated with the chromium (III)-based compound (IC_{50} dose at 800 μg/mL), oxaliplatin (IC_{50} dose at 35 μg/mL), and combination of chromium (III)-based compound and oxaliplatin. The SW620 cells were incubated with the chromium (III)-based compound (IC_{50} dose at 900 μg/mL), oxaliplatin (IC_{50} dose at 25 μg/mL), and combination of chromium (III)-based compound and oxaliplatin. The scale bar was 100 μm. The data are shown as the mean ± standard deviation (SD) of three replicates. *P < 0.05, **P < 0.01, and ***P < 0.001 compared with the control group of SW620 cells. #P < 0.05, ##P < 0.01, and ###P < 0.001 compared with the control group of HCT-116 cells.

Chromium (III)-based compound reduction in tumor development of CRC, leading to apoptosis in in-vitro and -vivo models

The potential of the chromium (III)-based compound to induce apoptosis in CRC cells was further investigated to expand the previously observed inhibitory effects of this compound on CRC cell viability, migration, and invasion. TUNEL assay was employed to assess the cell apoptosis in $LoVo^{parental}$ and $LoVo^{OXAR}$ cells following 24 h incubation with the chromium (III)-based compound at the concentrations of 500 μg/mL for $LoVo^{parental}$ cells and 2000 μg/mL for $LoVo^{OXAR}$ cells. The results demonstrated that the chromium (III)-based compound significantly increased the number of TUNEL-positive cells in both cell lines, highlighting its capability to induce CRC apoptosis (**Figure 8A** and **8B**).

Subsequently, xenograft experiments were conducted by implanting $LoVo^{parental}$ and $LoVo^{OXAR}$ tumor cells into nude mice and dividing them into four groups. Seven days after tumor inoculation, the treatment group was administered with 100 mg/kg of the chromium (III)-based compound every 5 days per week for 3 weeks. The nude mice were sacrificed after treatment. Their body weight and tumor volume were recorded on the day after they were injected with the $LoVo^{parental}$ and $LoVo^{OXAR}$ tumor cell lines (**Figure 8C** and **8E**). Based on tumor observation, the tumor volume treated with the chromium (III)-based compound significantly reduced (**Figure 8C** and **8D**). Further assessment using TUNEL assay on the $LoVo^{parental}$ and $LoVo^{OXAR}$ tumor tissue samples demonstrated that the chromium (III)-based compound significantly inhibited tumor development by inducing apoptosis, with images captured at a scale bar of 100 μm (**Figure 9A** and **9B**). The findings from the *in-vitro* and *in-vivo* models suggested that the chromium (III) based compound has the capacity to trigger apoptosis in $LoVo^{parental}$ and $LoVo^{OXAR}$ cells, highlighting its potential as a useful therapeutic agent in CRC.

Chromium (III)-based compound prompts cell death in drug-resistant CRC cells through the activation of the ER-stress pathway

How the chromium (III)-based compound induces cell death in drug-resistant CRC cells was determined. The PERK-eIF2α-ATF4-CHOP pathway is a central signaling pathway in mediating apoptosis induced by ER stress. Phosphorylation of eIF2α by PERK is a key event in this pathway, leading to the activation of ATF4 and then the induction of CHOP. This cascade of events is pivotal in orchestrating the apoptotic response during severe ER stress [38, 39]. The role of phosphorylated eIF2α (p-eIF2α) in inhibiting the synthesis of large quantities of proteins is particularly important. This inhibition is a critical aspect of impeding the tumorigenesis process [40]. In the present research, the lev-

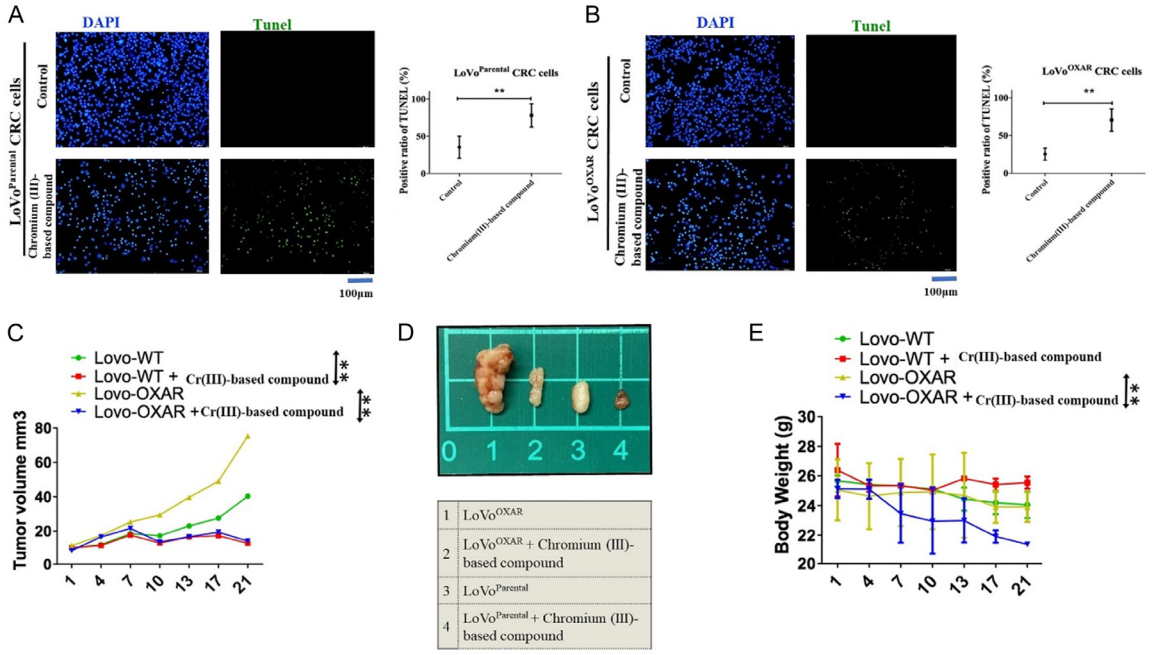

Figure 8. Antitumor activity of the chromium (III)-based compound via apoptosis induction in tumor development of colorectal cancer cell lines and animal models. A and B. TUNEL assay of apoptotic-positive cells marked by green staining in LoVo^{parental} cells treated with 500 μg/mL of chromium (III)-based compound and LoVo^{OXAR} cells treated with 2000 μg/mL of chromium (III)-based compound. The scale bar was 100 μm. **P < 0.01 compared with the control group. C. The tumor volume of nude mice was recorded on the day after the LoVo^{parental} or LoVo^{OXAR} cell lines were injected. **P < 0.01. D. Tumors were subcutaneously implanted in LoVo^{parental} and LoVo^{OXAR} cells. Representative pictures of tumor masses isolated while sacrificing nude mice are shown. E. The body weight of nude mice was recorded the day after LoVo^{parental} or LoVo^{OXAR} tumor cells were injected into nude mice. The data were shown as the mean ± standard deviation (SD). **P < 0.01.

els of PERK, p-eIF2α, original eIF2α, ATF4, and CHOP in the LoVo^{OXAR} cells exhibited minimal changes when treated with oxaliplatin compared with those of the untreated group. Furthermore, the LoVo^{OXAR} cells treated with oxaliplatin exhibited a decrease in the primary apoptotic regulator, cleaved caspase 3, compared with the untreated group, whereas the level of full-length PARP slightly decreased. However, the chromium (III)-based compound enhanced the expression levels of PERK, p-eIF2α, ATF4, and CHOP, resulting in increased cleaved caspase 3 and decreased full-length PARP levels. This phenomenon, in turn, facilitated cell death in LoVo^{OXAR} cells (**Figure 10**). The combination of the chromium (III)-based compound with oxaliplatin elicited a similar pattern in LoVo^{OXAR} cells. The results demonstrated that the chromium (III)-based compound triggers ER stress by activating several key proteins, including PERK, p-eIF2α, ATF4, CHOP, and caspase-3 protein cleavage leads to cell death in LoVo^{OXAR} cells. Therefore, the chromium (III)-based compound induces apoptosis by activating the ER stress pathway in drug-resistant CRC cells. Notably, this compound additionally initiated the cleavage of caspase 3, resulting in decreased PARP levels in LoVo^{parental} cells. On the contrary, the proteins in the PERK-eIF2α-ATF4-CHOP pathway showed less changes, suggesting that the compound may induce cell death in LoVo^{parental} cells through an alternative signaling pathway. This innovative chromium (III)-based compound holds promise as a novel treatment for CRC and exhibits the potential to effectively combat drug-resistant CRC cells.

Discussion

The prevalence of CRC is increasing, with over million individuals diagnosed each year, and the disease claims the lives of more around 9 million people annually. This type of cancer arises within the context of hereditary cancer syndromes or as a result of aging, unhealthy lifestyle, or other risk factors such as inflamma-

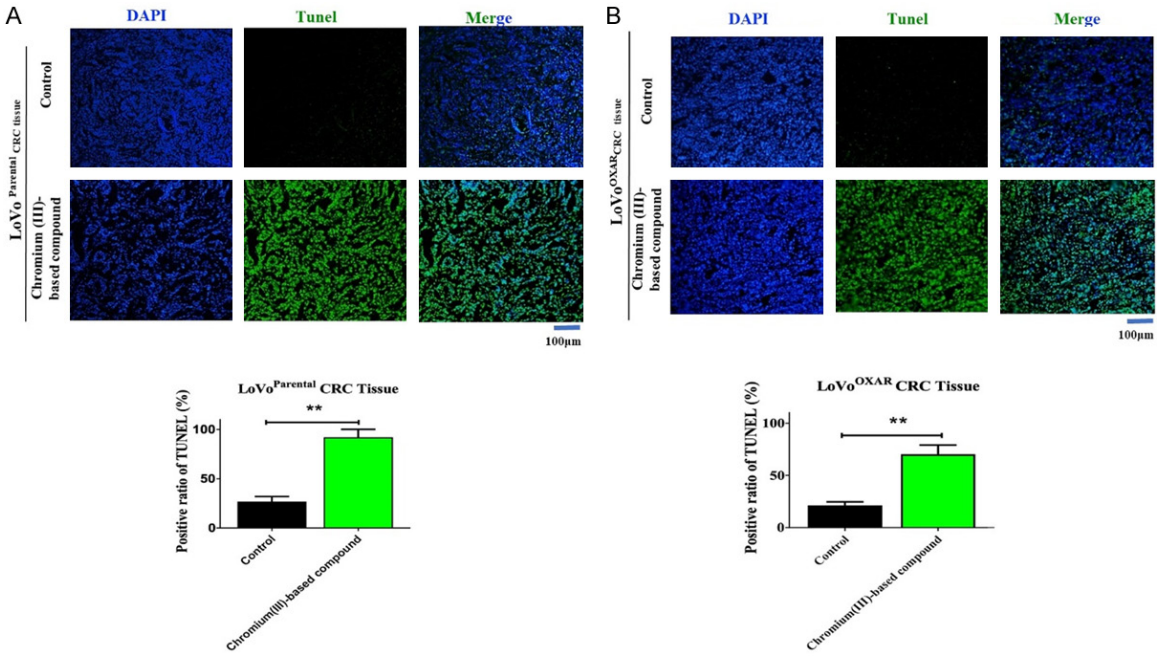

Figure 9. Reduction in tumor development by chromium (III)-based compound treatment through inducing apoptosis in LoVo^{parental} and LoVo^{OXAR} tumor tissue. A and B. TUNEL assay was conducted on the apoptotic marker in LoVo^{parental} and LoVo^{OXAR} tumor tissue samples with a scale bar of 100 μm. The data are shown as mean ± standard deviation (n = 3, each group). **P < 0.01 versus control.

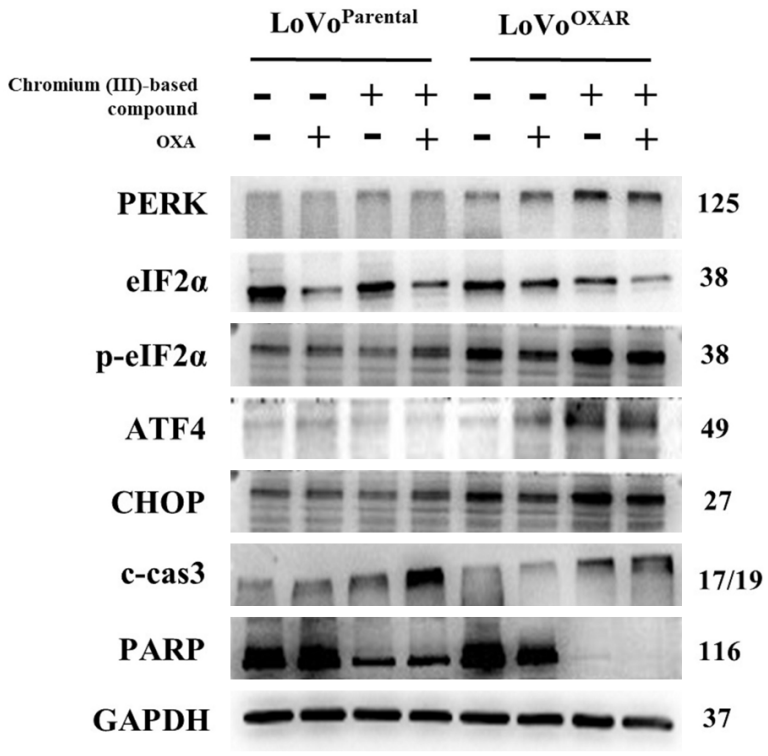

Figure 10. Chromium (III)-based compound-enhanced apoptosis in LoVo oxaliplatin-resistant colorectal cancer cells by activating ER stress pathway. The phosphorylation levels of eIF2α, PERK, ATF4, and CHOP, which are ER-stress protein markers, increased, resulting in an increase in cleaved caspase 3 and a decrease in full-length PARP, ultimately leading to apoptosis. All proteins were analyzed by Western blot. GAPDH was used as an internal control.

tory bowel disease. Several different therapies, such as chemotherapy, radiotherapy, and molecularly targeted therapies, could improve the prognosis of patients with CRC [41]. However, the efficacy of these drugs is substantially compromised by the development of drug resistance.

Trivalent chromium is recognized as a vital trace element for mammals. While the current consensus on the essentiality of chromium in the human body is under debate, with some considering it a non-essential element, ongoing research suggests that chromium (III) compound may still manifest potential pharmacological effects [42]. Previous anti-CRC research highlighted that a chromium (III) compound called $[Cr_3O(O_2CCH_2CH_3)_6(H_2O)_3]^+$ provides benefits for insulin sensitivity and serum lipids,

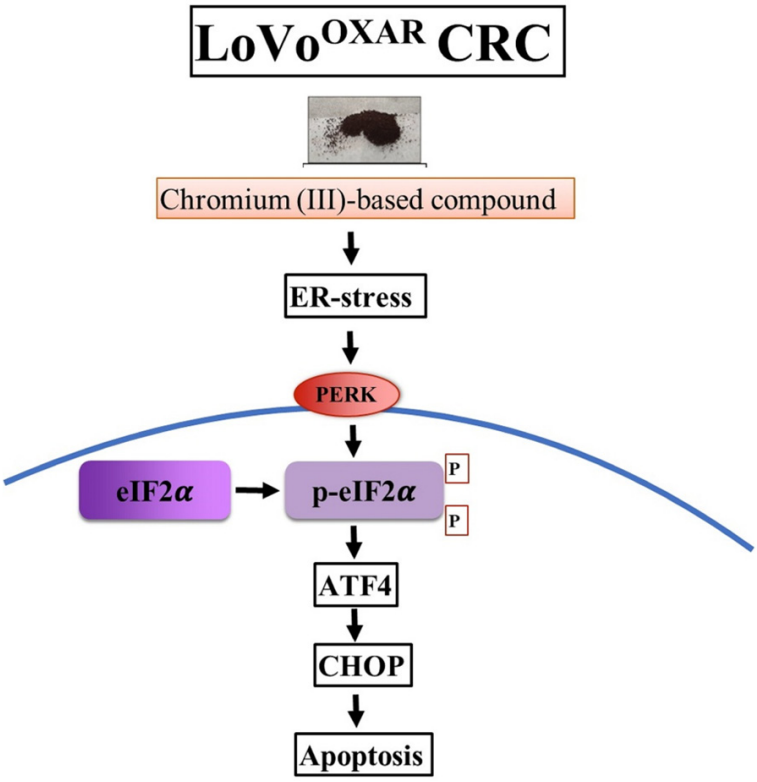

Figure 11. Schematic of chromium (III)-based compound-induced apoptosis in LoVo oxaliplatin-resistant colorectal cancer cells via activation of ER stress pathway.

consequently lowering the risk of CRC in a rat model [18]. Therefore, compounds derived from chromium (III) hold the potential to mitigate the risk of CRC. In the current research, a newly synthesized chromium (III)-based compound with the chemical formula $[CrFe_2(CH_3CO_2)_6(H_2O)_4(OH)_2]^+NO_3^-$, designated as hexaacetotetraaquadihydroxochromium (III) diiron (III) nitrate, was studied as a prospective therapeutic agent in the fight against CRC and to address resistance to chemotherapy.

In the present study, our findings indicate that the recently developed chromium (III)-based compound exhibits lower cytotoxicity in normal cell lines (Beas-2B and H9c2 cell lines). However, it inhibited cell viability in several different CRC cell lines, and a high dose was required for oxaliplatin-resistant CRC cells to reduce cell viability. Notably, the synergistic effect of the chromium (III)-based compound in combination with oxaliplatin or other chemotherapeutic drugs (5-FU and irinotecan) substantially augmented the effectiveness of these chemotherapeutic agents in LoVo^{parental} and LoVo^{OXAR} cells. Invasion and migration are pivotal activities in tumor progression. Further investigation unveiled that the chromium (III)-based compound influenced various markers associated with EMT, which is known to aggravate tumor development and metastasis. Cells undergoing EMT extend beyond and break down the surrounding microenvironment prior to migrating from the primary site [43]. The findings of the present study demonstrated that the chromium (III)-based compound inhibited the migration and invasion capabilities of CRC cells in the presence and absence of oxaliplatin resistance. Notably, the levels of E-cadherin and TJP1, both recognized as tumor suppressors that tend to diminish during cancer development, significantly increased [31, 32, 44]. Meanwhile, the vimentin and FN1 levels decreased following treatment with the chromium (III)-based compound. Both are key components of the intermediate filament family of proteins associated with enhancing cancer progression [28, 36, 37, 45]. Additionally, whether the chromium (III)-based compound has the ability to induce apoptosis was investigated. TUNEL assay was employed to assess cell apoptosis, revealing a substantial induction of apoptosis in both CRC cell lines by the chromium (III)-based compound. A tumor xenograft study in nude mice treated with the chromium (III)-based compound (100 mg/kg body weight) for 3 weeks demonstrated a significant reduction in tumor development and an increase in cell apoptosis within the tissue. Although consistent body weights were observed across groups, except in the group with drug-resistant tumor treated with the chromium (III)-based compound, all mice remained healthy after treatment with the compound. The finding indicated that this innovative chromium (III)-based compound exhibits antitumor activity in tumor progression and development, proving to be beneficial for colon health.

The onset of tumor development, arising from various cellular stress conditions, can instigate

disturbances in ER homeostasis, thereby inducing ER stress. The PERK/eIF2α/ATF4 pathway assumes a pivotal role in cancer cells experiencing ER stress. ER stress initiates PERK activation through phosphorylation, subsequently triggering the phosphorylation of eIF2α and then leading to an upregulation in ATF4 levels. In an adaptive response, ATF4 orchestrates the expression of cytoprotective proteins, thereby enhancing tumor growth. However, when cancer cells experience prolonged ER stress, they undergo programmed cell death. In the apoptotic response, ATF4 activates CHOP, thus promoting apoptosis [39]. Our previous study confirmed that the attenuation of ER stress reduced apoptosis in LoVo CRC cells with oxaliplatin resistance [10]. In the current study, the expression levels of proteins associated with tumor progression and development, such as PARP, decreased, whereas the proteins linked to the inhibition of tumor development and apoptosis, including PERK, phosphorylated eIF2α, ATF4, CHOP, and caspase-3, showed an increase in $LoVo^{OXAR}$ CRC cells. These results suggested that the ER stress induced by the chromium (III)-based compound may trigger the PERK/eIF2α/ATF4/CHOP pathway, leading to apoptosis in $LoVo^{OXAR}$ CRC cells. This confirmation supports the promising role of the chromium (III)-based compound against the development of drug-resistant CRC cells.

While all the findings affirmed the anti-CRC potential of the chromium (III)-based compound, underscoring the limitations of this study is crucial. First, the validation of the findings requires the inclusion of additional drug-resistant CRC cell lines. Second, the mechanism of cell death induction in $LoVo^{parental}$ cells requires further investigation to further understand the efficacy of this compound in CRC. A toxicity study in animals is essential to further validate the safety profile of this compound prior to progressing to clinical trials. Even though the present study has some limitations, the findings still demonstrated that this novel chromium (III)-based compound exhibits antitumor activity, enhances the effectiveness of clinical drugs synergistically, and impedes the progression of oxaliplatin resistance in CRC. This study suggests the potential of the chromium (III)-based compound as a therapeutic agent for CRC, even in the face of drug resistance.

Conclusion

This study revealed that the novel chromium (III)-based compound plays a crucial role in preventing metastasis and suppressing tumor progression in chemotherapy-resistant CRC. The results demonstrated that this compound reduces the EMT protein levels, thus influencing metastatic ability, migration, and invasion. The chromium (III)-based compound also caused apoptosis of CRC cells in the *in-vitro* and *in-vivo* models and induced apoptosis in drug-resistant CRC cells through the ER stress pathway (**Figure 11**). The findings suggest that the chromium (III)-based compound holds the potential to contribute to the treatment of primary therapy and chemotherapy-resistant CRC in the future.

Acknowledgements

This research was supported by Miss Feng-Mei Wen and the Chairman of TOMA Biotechnology. We thank our colleagues at TOMA BIO. Co., Ltd., who provided insight and expertise that greatly assisted this research. We thank the fundings provided by Hualien Tzu Chi Hospital (TCRD-112-074), National Science and Technology Council, Taiwan (NSTC 111-2811-B-303-006, NSTC 112-2811-B-303-003, and NSTC 112-2320-B-303-002), and Ministry of Science and Technology, Taiwan (MOST 111-2314-B-303-008-MY3).

Disclosure of conflict of interest

The innovative chromium (III)-based compound was provided by TOMA BIO. Co., Ltd. (Taipei, Taiwan).

Abbreviations

CRC, Colorectal cancer; EMT, Epithelial-Mesenchymal Transition; ER, Endoplasmic Reticulum; OXA, Oxaliplatin; RT-PCR, Real-Time PCR.

Address correspondence to: Drs. Yu-Jung Lin and Chih-Yang Huang, Cardiovascular and Mitochondrial Related Disease Research Center, Hualien Tzu Chi Hospital, Buddhist Tzu Chi Medical Foundation, Hualien, Taiwan. Tel: +886-3-8561825 Ext. 15730; Fax: +886-4-22032295; E-mail: u9882851@gmail.com (YJL); Tel: +886-3-8561825 Ext. 15930; Fax: +886-4-22032295; E-mail: cyhuang@mail.cmu.edu.tw (CYH)

References

[1] Thanikachalam K and Khan G. Colorectal cancer and nutrition. Nutrients 2019; 11: 164.

[2] Köberle B and Schoch S. Platinum complexes in colorectal cancer and other solid tumors. Cancers (Basel) 2021; 13: 2073.

[3] Meyerhardt JA and Mayer RJ. Systemic therapy for colorectal cancer. N Engl J Med 2005; 352: 476-487.

[4] Kelland L. The resurgence of platinum-based cancer chemotherapy. Nat Rev Cancer 2007; 7: 573-584.

[5] Alcindor T and Beauger N. Oxaliplatin: a review in the era of molecularly targeted therapy. Curr Oncol 2011; 18: 18-25.

[6] Hsu HH, Kuo WW, Shih HN, Cheng SF, Yang CK, Chen MC, Tu CC, Viswanadha VP, Liao PH and Huang CY. FOXC1 regulation of miR-31-5p confers oxaliplatin resistance by targeting LATS2 in colorectal cancer. Cancers (Basel) 2019; 11: 1576.

[7] Evert J, Pathak S, Sun XF and Zhang H. A study on effect of oxaliplatin in microRNA expression in human colon cancer. J Cancer 2018; 9: 2046-2053.

[8] Sun W, Ge Y, Cui J, Yu Y and Liu B. Scutellarin resensitizes oxaliplatin-resistant colorectal cancer cells to oxaliplatin treatment through inhibition of PKM2. Mol Ther Oncolytics 2021; 21: 87-97.

[9] Zhang Y, Li C, Liu X, Wang Y, Zhao R, Yang Y, Zheng X, Zhang Y and Zhang X. circHIPK3 promotes oxaliplatin-resistance in colorectal cancer through autophagy by sponging miR-637. EBioMedicine 2019; 48: 277-288.

[10] Hsu HH, Chen MC, Baskaran R, Lin YM, Day CH, Lin YJ, Tu CC, Vijaya Padma V, Kuo WW and Huang CY. Oxaliplatin resistance in colorectal cancer cells is mediated via activation of ABCG2 to alleviate ER stress induced apoptosis. J Cell Physiol 2018; 233: 5458-5467.

[11] Chen MC, Yang BZ, Kuo WW, Wu SH, Wang TF, Yeh YL, Chen MC and Huang CY. The involvement of Aurora-A and p53 in oxaliplatin-resistant colon cancer cells. J Cell Biochem 2023; 124: 619-632.

[12] Genchi G, Lauria G, Catalano A, Carocci A and Sinicropi MS. The double face of metals: the intriguing case of chromium. Applied Sciences 2021; 11: 638.

[13] Deng Y, Wang M, Tian T, Lin S, Xu P, Zhou L, Dai C, Hao Q, Wu Y, Zhai Z, Zhu Y, Zhuang G and Dai Z. The effect of hexavalent chromium on the incidence and mortality of human cancers: a meta-analysis based on published epidemiological cohort studies. Front Oncol 2019; 9: 24.

[14] Havel PJ. A scientific review: the role of chromium in insulin resistance. Diabetes Educ 2004; Suppl: 2-14.

[15] Li P, Cao Y, Song G, Zhao B, Ma Q, Li Z and He C. Anti-diabetic properties of genistein-chromium (III) complex in db/db diabetic mice and its sub-acute toxicity evaluation in normal mice. J Trace Elem Med Biol 2020; 62: 126606.

[16] Cui J, Gu X, Wei Z, Qiao L, Chunying D, Wang J, Liu R and Wang P. Hypolipidemic activity and safety evaluation of a rhamnan-type sulfated polysaccharide-chromium (III) complex. J Trace Elem Med Biol 2022; 72: 126982.

[17] Chen M, Huang X, Shi H, Lai J, Ma L, Lau TC and Chen T. Cr(V)-Cr(III) in-situ transition promotes ROS generation to achieve efficient cancer therapy. Biomaterials 2021; 276: 120991.

[18] Pickering A, Chang C and Vincent JB. Chromium-containing biomimetic cation triaqua-mu3-oxo-mu-hexapropionatotrichromium (III) inhibits colorectal tumor formation in rats. J Inorg Biochem 2004; 98: 1303-1306.

[19] Lin YJ, Sundhar N, Devi HS, Pien HF, Wen SF, Sheu JL, Tsai BC and Huang CY. Development and evaluation of a novel chromium III-based compound for potential inhibition of emerging SARS-CoV-2 variants. Heliyon 2023; 9: e20011.

[20] Fang CW, Yang JS, Chiang JH, Shieh PC, Tsai FJ, Tsai CW and Chang WS. Metformin induces autophagy of cisplatin-resistant human gastric cancer cells in addition to apoptosis. Biomedicine (Taipei) 2023; 13: 14-23.

[21] Chang WS, Tsai CW, Yang JS, Hsu YM, Shih LC, Chiu HY, Bau DT and Tsai FJ. Resveratrol inhibited the metastatic behaviors of cisplatin-resistant human oral cancer cells via phosphorylation of ERK/p-38 and suppression of MMP-2/9. J Food Biochem 2021; 45: e13666.

[22] Achudhan D, Li-Yun Chang S, Liu SC, Lin YY, Huang WC, Wu YC, Huang CC, Tsai CH, Ko CY, Kuo YH and Tang CH. Antcin K inhibits VCAM-1-dependent monocyte adhesion in human rheumatoid arthritis synovial fibroblasts. Food Nutr Res 2022; 66.

[23] Zeynali P, Jazi MS, Asadi J and Jafari SM. A1 adenosine receptor antagonist induces cell apoptosis in KYSE-30 and YM-1 esophageal cancer cell lines. Biomedicine (Taipei) 2023; 13: 54-61.

[24] Lu SY, Hong WZ, Tsai BC, Chang YC, Kuo CH, Mhone TG, Chen RJ, Kuo WW and Huang CY. Angiotensin II prompts heart cell apoptosis via AT1 receptor-augmented phosphatase and tensin homolog and miR-320-3p functions to enhance suppression of the IGF1R-PI3K-AKT survival pathway. J Hypertens 2022; 40: 2502-2512.

[25] Lai CH, Van Thao D, Tsai BC, Hsieh DJ, Chen MY, Kuo WW, Kuo CH, Lu SY, Liao SC, Lin KH and Huang CY. Insulin-like growth factor II receptor alpha overexpression in heart aggravates hyperglycemia-induced cardiac inflam-

mation and myocardial necrosis. Environ Toxicol 2023; 38: 676-684.
[26] Liu SP, Shibu MA, Tsai FJ, Hsu YM, Tsai CH, Chung JG, Yang JS, Tang CH, Wang S, Li Q and Huang CY. Tetramethylpyrazine reverses high-glucose induced hypoxic effects by negatively regulating HIF-1α induced BNIP3 expression to ameliorate H9c2 cardiomyoblast apoptosis. Nutr Metab (Lond) 2020; 17: 12.
[27] Feng B, Dong TT, Wang LL, Zhou HM, Zhao HC, Dong F and Zheng MH. Colorectal cancer migration and invasion initiated by microRNA-106a. PLoS One 2012; 7: e43452.
[28] Satelli A and Li S. Vimentin in cancer and its potential as a molecular target for cancer therapy. Cell Mol Life Sci 2011; 68: 3033-3046.
[29] Mendonsa AM, Na TY and Gumbiner BM. E-cadherin in contact inhibition and cancer. Oncogene 2018; 37: 4769-4780.
[30] Wijshake T, Zou Z, Chen B, Zhong L, Xiao G, Xie Y, Doench JG, Bennett L and Levine B. Tumor-suppressor function of Beclin 1 in breast cancer cells requires E-cadherin. Proc Natl Acad Sci U S A 2021; 118: e2020478118.
[31] Zhang B, Chan SH, Liu XQ, Shi YY, Dong ZX, Shao XR, Zheng LY, Mai ZY, Fang TL, Deng LZ, Zhou DS, Chen SN, Li M and Zhang XD. Targeting hexokinase 2 increases the sensitivity of oxaliplatin by Twist1 in colorectal cancer. J Cell Mol Med 2021; 25: 8836-8849.
[32] Li M, Zhou DS, Shao XR, Chan SH, Dong ZX, Liu XQ, Chen SN, Qi L, Zarate LV, Wang XM, Du X and Zhang XD. Tight junction protein 1 suppresses kidney renal clear cell carcinoma cells proliferation by inducing autophagy. Int J Med Sci 2023; 20: 1448-1459.
[33] Lee EY, Kim M, Choi BK, Kim DH, Choi I and You HJ. TJP1 contributes to tumor progression through supporting cell-cell aggregation and communicating with tumor microenvironment in leiomyosarcoma. Mol Cells 2021; 44: 784-794.
[34] Lee YC, Tsai KW, Liao JB, Kuo WT, Chang YC and Yang YF. High expression of tight junction protein 1 as a predictive biomarker for bladder cancer grade and staging. Sci Rep 2022; 12: 1496.
[35] Chong X, Peng R, Sun Y, Zhang L and Zhang Z. Identification of key genes in gastric cancer by bioinformatics analysis. Biomed Res Int 2020; 2020: 7658230.
[36] Steffens S, Schrader AJ, Vetter G, Eggers H, Blasig H, Becker J, Kuczyk MA and Serth J. Fibronectin 1 protein expression in clear cell renal cell carcinoma. Oncol Lett 2012; 3: 787-790.
[37] Xia S, Wang C, Postma EL, Yang Y, Ni X and Zhan W. Fibronectin 1 promotes migration and invasion of papillary thyroid cancer and predicts papillary thyroid cancer lymph node metastasis. Onco Targets Ther 2017; 10: 1743-1755.
[38] Pandey VK, Mathur A, Khan MF and Kakkar P. Activation of PERK-eIF2α-ATF4 pathway contributes to diabetic hepatotoxicity: attenuation of ER stress by Morin. Cell Signal 2019; 59: 41-52.
[39] Rozpedek W, Pytel D, Mucha B, Leszczynska H, Diehl JA and Majsterek I. The role of the PERK/eIF2α/ATF4/CHOP signaling pathway in tumor progression during endoplasmic reticulum stress. Curr Mol Med 2016; 16: 533-544.
[40] Guo L, Chi Y, Xue J, Ma L, Shao Z and Wu J. Phosphorylated eIF2α predicts disease-free survival in triple-negative breast cancer patients. Sci Rep 2017; 7: 44674.
[41] Dekker E, Tanis PJ, Vleugels JLA, Kasi PM and Wallace MB. Colorectal cancer. Lancet 2019; 394: 1467-1480.
[42] Vincent JB. New evidence against chromium as an essential trace element. J Nutr 2017; 147: 2212-2219.
[43] Smith BN and Bhowmick NA. Role of EMT in metastasis and therapy resistance. J Clin Med 2016; 5: 17.
[44] Gottardi CJ, Wong E and Gumbiner BM. E-cadherin suppresses cellular transformation by inhibiting beta-catenin signaling in an adhesion-independent manner. J Cell Biol 2001; 153: 1049-1060.
[45] Xie Y, Liu C, Qin Y, Chen J and Fang J. Knockdown of IRE1α suppresses metastatic potential of colon cancer cells through inhibiting FN1-Src/FAK-GTPases signaling. Int J Biochem Cell Biol 2019; 114: 105572.